

Calibration and characterization of photomultiplier tubes of the IceCube neutrino detector

H. Miyamoto^a for the IceCube collaboration

(a) *Dept. of Physics, Chiba University, Chiba 263-8522 Japan*

Presenter: H. Miyamoto (miya@hepburn.s.chiba-u.ac.jp), jap-miyamoto-H-abs1-og25-poster

The IceCube neutrino observatory will consist of an InIce array of 4800 Digital Optical Modules (DOMs) located in the deep ice at the South Pole, and also an IceTop air shower array of 320 DOMs in 160 ice tanks located on the surface. A 10 inch PMT is housed in each DOM for the detection of Cherenkov light. This paper describes the methods of calibration and characterization of the IceCube PMTs in the laboratory, which are germane to improving the detector resolution and reducing systematic uncertainties. Two dimensional scans on the entire photocathode to map out photon conversion efficiency have been carried out for 60 PMTs. The quantum/collection efficiency has been calibrated in an absolute manner using the Rayleigh scattered light from our newly built chamber filled with nitrogen gas. The charge response of the PMTs at temperatures below freezing has been extensively studied and found to be well represented by the analytical model. All these results have been combined and implemented in the detector Monte Carlo simulation.

1. Introduction

IceCube[1] is a high energy cosmic neutrino detector which will instrument a cubic kilometer of ice sheet covering the South Pole. The InIce DOMs will be deployed on eighty strings of sixty DOMs each, and these strings will be regularly spaced by 125 m over an area of approximately one square kilometer, with the DOMs at depths ranging from 1.4 km to 2.4 km below the ice surface. An IceCube event consists of Cherenkov photon profiles recorded in individual DOMs in the form of digitized waveform output from the PMT. An accurate understanding of the PMT response is, therefore, necessary in order to determine both the geometry of these events as well as to reconstruct their energies. Moreover, having carefully calibrated PMTs would lead to a significant reduction of systematic uncertainties because it is of great help in characterizing the optical properties of glacial ice more accurately. In this paper we describe our relative and absolute calibration of the IceCube PMTs. Their charge responses and photon detection efficiencies are measured and implemented in the detector Monte Carlo simulation.

2. The IceCube Optical Detector: DOM

Each DOM contains a 10 inch diameter PMT supported by coupling gel, a signal processing electronics board, an LED flasher board for calibration, and a high voltage base which powers the PMT, all of which are housed in a glass pressure sphere. It contains its own processor, memory, flash file system, and real-time operating system. Its new digital technology enables it to schedule communications in the background while acquiring data, to invoke all calibration functions under software control, and most notably, to digitize the PMT pulse and store the full waveform information.

The IceCube PMT is the Hamamatsu R7081-02 with 10 dynodes. This PMT exhibits excellent charge resolution and low noise. The PMTs in InIce DOMs are operated nominally at a gain of $\sim 1 \times 10^7$. They exhibit an excellent peak to valley ratio (≥ 2.0) and remarkably low dark count rate ($\sim 500 Hz$) at sub-freezing temperatures, both of which have a significant impact on the performance of the IceCube detector.

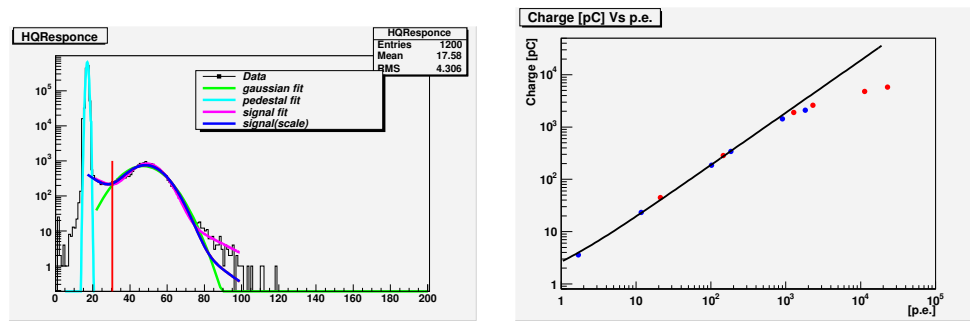


Figure 1. Left panel: The charge histogram with the fitted SPE model function. Right panel: PMT linearity data. The output charge is plotted as a function of the number of photoelectrons corresponding to the LED luminosity. The PMT gain is 1.2×10^7 .

3. Fundamental PMT calibration in a freezer

The basic behavior of the PMTs at sub-freezing temperatures should be well understood. A PMT put in a freezer box is illuminated by diffuse light from a UV LED for measuring the PMT gain, single photoelectron (SPE) response, and dark count rate. An SPE waveform has been found to be represented well by a gaussian with $\sigma \sim 2$ nsec. Dark count rates above a trigger threshold of 0.3 PE were found to be distributed around 600 Hz for PMTs with a gain of 5×10^7 . This corresponds to ~ 470 Hz at the operating gain of 1×10^7 .

The charge response for SPE detection has been extensively studied. In general it is assumed that the charge of an SPE pulse follows a gaussian distribution. However, a large PMT like those used in IceCube is occasionally observed to fail to stream secondary electrons out from the first to the second dynode, which results in a non-gaussian response. Here the charge response of the IceCube PMTs is modeled by an exponential term in conjunction with the widely-used gaussian term. Figure 1 in the left panel illustrates how well this model function represents the charge histogram. One of the advantages in this model representation is that the scaling law to PMT gain appears valid in the model function. The relevant model parameters are recorded into a database, which is used by the detector Monte Carlo simulation.

It is also important to measure the linearity of the PMT response to multiple photoelectrons. A bright LED with a set of calibrated neutral density filters is used to provide various luminosities of UV photons for such a linearity measurement. The result is shown in the right panel of Figure 1. The number of photoelectrons is estimated from the SPE peak and the attenuation factor of each filter. It is found that an IceCube PMT has a linear response up to approximately one thousand photoelectrons at the gain of $\sim 1 \times 10^7$. Since a representative FWHM of the LED light pulse is 30 nsec in this measurement, the corresponding current where the PMT deviates from the linear response is ~ 60 mA.

4. Two dimensional photocathode scan

The IceCube PMT collects photoelectrons generated in its relatively large cathode area and its efficiency depends on the position on the cathode surface. Moreover, the variance of the electric field inside the tube to collect photoelectrons at the dynode gives non-negligible differences in the charge collection efficiency from tube to tube. We have systematically analyzed the dependency of the overall PMT efficiency on the photocathode position, using a two dimensional scan system. A UV LED moves along the curved PMT surface to scan the entire photocathode. The light beam is controlled to be precisely perpendicular to the cathode glass. A collimator attached in front of the LED gives a spot size of ~ 1 mm. The light spot pointing accuracy is ≤ 4.8 mm which is sufficient to scan the cathode with its radius of ~ 14 cm.

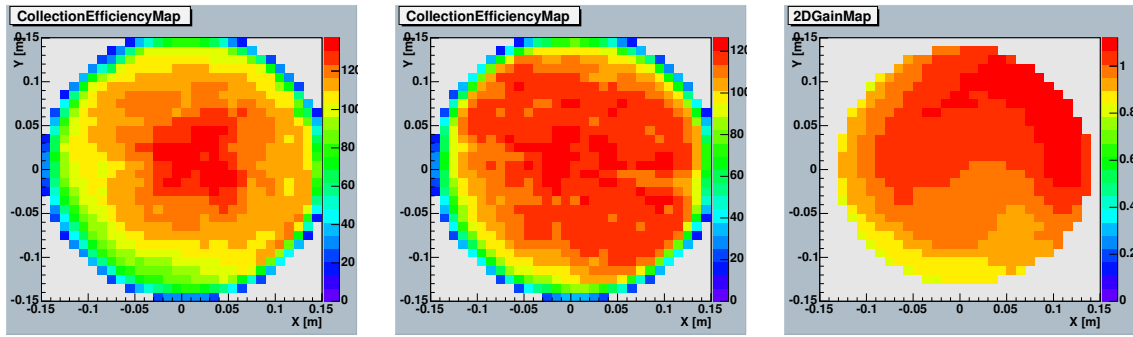


Figure 2. Left and middle panels: Examples of the position dependence of the collection efficiency. The relative collection efficiency is mapped in the XY plane for two different PMTs. Right panel: An example of the normalized position dependence of the PMT relative gain where the average gain over the cathode is 1.0.

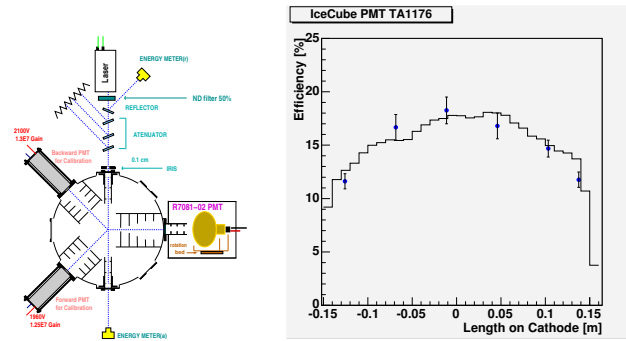


Figure 3. Left panel: Schematic view of the absolute calibration system. Right panel: The detection efficiency for photons with a wavelength of 337 nm for one of the IceCube PMTs. The efficiency is plotted as a function of the distance from the cathode center. The light spot size is approximately 1.0 cm. The histogram shows the two dimensional scan data described in Section 4, after applying the appropriate normalization.

Figure 2 shows some examples. A relative collection efficiency is shown as a function of the projected X-Y location on the cathode surface. A shield made of μ -Metal is used to negate the geomagnetic field inside the PMT. From measuring the effects of rotating a PMT it was determined that the systematic uncertainty due to the geomagnetic field was $\sim 5\%$. On average, an IceCube PMT exhibits non-uniformity at a level of $\sim 7\%$. However, variations from PMT to PMT have been found to be $\sim 40\%$. It is therefore necessary to evaluate how these variations would influence the detector resolution. The measured data has been integrated into the detector simulation for such a study.

In contrast to the collection efficiency, the gain should be rather uniform. Scanning the PMT using a dim LED provides an SPE-based gain map along the photocathode surface. The right panel of Figure 2 shows an example. The actual (absolute) gain for this particular PMT is approximately 4.4×10^7 . As expected, it is quite uniform compared to the collection efficiency. Moreover, there is no significant variation from PMT to PMT. The gain uniformity behavior can be considered universal among the IceCube PMTs, which simplifies the detector response simulation.

Table 1. The evaluated absolute photon detection efficiency for 4 different PMTs.

PMT number	$Q_{eff}^{center}(q_{th} = 0.5p.e.)$	$Q_{eff}^{whole}(q_{th} = 0.5p.e.)$	$Q_{eff}^{whole}(q_{th} = 0.0p.e.)$	Error (stat)
TA1052	19.4 %	16.4 %	23.5 %	± 1.3 %
TA1062	19.2 %	16.7 %	22.9 %	± 1.3 %
TA1176	17.5 %	13.9 %	19.7 %	± 1.2 %
TA1167	18.2 %	16.4 %	22.9 %	± 1.3 %

5. Absolute calibration

The left panel of Figure 3 illustrates our absolute calibration system. A tiny fraction of laser beam photons are scattered inside the pressurized chamber filled with nitrogen gas. A pressure gauge and a temperature sensor estimate the density of the gas. The laser beam energy is measured by the silicon energy meter. Because the wavelength of the laser photon is a monochromatic 337 nm, this energy can be converted to the number of photons injected by the laser. Only photons with scatter angles of $\sim 90^\circ$ will reach the IceCube PMT photocathode to provide an SPE signal, while scattered photons in the other directions will eventually be absorbed by a number of baffles inside the chamber. The spot size of scattered photons which illuminate the PMT cathode is approximately 1.5 cm. The PMT is rotated inside the dark box so that the detection efficiency can be measured from position to position on the photocathode surface. The number of scattered photons which reach the PMT cathode, N_γ , is determined by the geometrical acceptance of the PMT, the well-understood Rayleigh scattering cross section, the number density of the nitrogen gas, and the number of photons injected by the laser.

The average number of photoelectrons N_{pe} detected by a PMT is obtained from the ratio of the number of SPE and multiple photoelectron events N_{SPE} to all events externally triggered by the synchronized gate pulse from the laser. Our definition of an SPE event here is those events which produce charge q greater than $q_{th} = 0.5$ photoelectrons, which can be clearly discriminated in the charge histogram taken by the CAMAC ADC. It should be noted, however, that our charge response model is capable of evaluating $N_{SPE}(q_{th})$ with a lower threshold than 0.5 photoelectrons, since it provides the probability of an SPE signal as a function of charge. The PMT photon detection efficiency is then calculated from N_{pe} and N_γ . The relative statistical and systematic errors, $\Delta Q_{eff}/Q_{eff}$ of the present calibration are ~ 5 % and ~ 7 %, respectively.

The data points in the right panel of figure 3 show the determined detection efficiency Q_{eff} as a function of the distance from the cathode center. The detection efficiency in the central area of the photocathode is measured to be 18 - 20 %. This is consistent with measurements by Hamamatsu which are based on DC light exposure. The histogram in figure 3 shows the two dimensionally scanned relative collection efficiency. The locally measured Q_{eff} data points agree very well with this histogram. Consequently, this allows us to estimate the averaged Q_{eff} over a certain area of the photocathode surface. Table 1 shows Q_{eff} in the central point and those averaged over the entire photocathode.

As mentioned earlier, the charge response model for calibrating PMTs in the dark freezer box described in Section 3 can determine Q_{eff} with lower thresholds of photoelectron charge. The non-biased efficiency $Q_{eff}(q_{th} = 0.0p.e.)$ would be a useful quantity in implementing the detector Monte Carlo simulation and these values are also listed in the table.

References

- [1] S. Yoshida 28th ICRC, Tsukuba (2003) 1369; K. Woschnagg, Nucl.Phys.B 143 (2005) 343;